2012

A Hybrid Photovoltaic-Thermal Energy Solar System

Suming Guo
Lehigh University

A HYBRID PHOTOVOLTAIC-THERMAL ENERGY SOLAR SYSTEM

by

Suming Guo

A Thesis

Presented to the Graduate and Research Committee

of Lehigh University

in Candidacy for the Degree of

Master of Science

in

Mechanical Engineering and Mechanics

Lehigh University

September 2012

This thesis is accepted and approved in partial fulfillment of the requirements for the Master of Science.

_____

Date Approved

_____

Dr. Sudhakar Neti, Thesis Advisor

_____

Dr. D. Gary Harlow, Chairperson of Department

Acknowledgments

This thesis would not have been possible without contributions from others.

First, I would like to thank my advisor, Professor Neti for his continued patience whenever I had any academic problems with this thesis. I determined my career goals after taking the renewable energy course taught by Professor Neti. I would also like to sincerely thank him for taking an interest in and offering advice about my life outside of academia. I am also grateful to the rest of the professors who helped me finish the core courses, such as Professors Kazakia and Oztekin. Finally, I would like to thank my family and friends for their continued support throughout my educational career. I would especially like to thank my parents for their encouragement and their belief in me.

TABLE OF CONTENTS

Acknowledgments iii

TABLE OF CONTENTS iv

LIST OF TABLES v

LIST OF FIGURES vi

ABSTRACT 1

CHAPTER 1. INTRODUCTION 2

1.1 Need for Renewable Energy 2
1.2 A Brief History about Solar Energy Utilization 3
CHAPTER 2. BACKGROUND AND PAST WORK OF PV/T SYSTEMS 5

2.1 Solar Radiation 5
2.1.1 Principal Features of the Sun 5
2.1.2 The Solar Constant 6
2.1.3 Extraterrestrial and Terrestrial Solar Radiation 7
2.2 Semiconductors Physics and Solar Cells 8
2.2.1 Energy Band Structure 9
2.2.2 Electrons and Holes 10
2.2.3 P-N Junction Diode Electrostatics 11
2.2.4 Solar Cell I-V Characteristics 13
2.3 Introduction of Current Hybrid Solar System 14
CHAPTER 3. A NEW TYPE OF CPV/T SYSTEM 19

3.1 Performance of the notch Filter 19
3.2 Performance of Parabolic Concentrators 20
3.2 Cavity Receiver 21
CHAPTER 4. EVAULATION OF CPV/T DISH 23

4.1 Solar Radiation Estimation in New York City 23
4.2 Efficiency Calculation for CPV/T Dish 24
CHAPTER 5. ENERGY ANALYSIS OF THE CPV/T DISH 31

5.1 Photovoltaic System Configurations 31
5.2 Solar Energy System Simulation for Household 34
CHAPTER 6. CONCLUSIONS 40

REFERENCE 42

Vita 44

LIST OF TABLES

Table 2.1 Representative Photovoltaic Material Band Gap Energies 9
Material 9
Table 4.1 Monthly Global, Beam and Diffuse Irradiance in New York City 24
Table 5.1 Electricity Daily Consumption Estimation for A Four People Family 35
Table 5.2 Specifications of Shell St40 36
Table 5.3 Energy Produced by PV Array and Consumption by A Four people family monthly 37
Table 5.4 Received Power by Cavity and Output Temperature Monthly 38

LIST OF FIGURES

Figure 1-1 Percentage Contributions of Energy Sources in 2007 2
Figure 1-2 Percentage Contributions of Renewable Energy in 2007 3
Figure2-1 Principal Features of The Sun 6
Figure 2-2 An Example of The Effects of Raleigh Scattering and Atmospheric Absorption on The Spectral Distribution of Beam Irradiance. 8
Figure 2-3 Energy Band Structure 9
Figure 2-4 P-N Junction Model 11
Figure 2-5 Simple Solar Cell Structure 12
Figure 2-6 Simple Solar Cell Circuit Model 14
Figure 2-8 Typical Sheet and Tube PV/T Collector 16
Figure 3-1 A New Type Hybrid Solar System 19
Figure 4-1 Global Spectral Irraidance At AM=1.5 25
Figure 4-2 Shockley- Queisser Efficiency Limit as A Function of Bandgap 26
Figure 4-3 Spectrum Distribution with The Photon Wavelength Between 800 nm And 1,120 nm 27
Figure 4-4 Current-Voltage Characteristic for Spectrally Selective Concentrated Photovoltaic (cpv) and Non-concentrated Solar Cells 29
Figure 5-1 Schematic of Direct Couple Systems 31
Figure 5-2 Schematic of Self- Regulated Systems 32
Figure 5-3 Schematic of Charge- Controlled Systems 32
Figure 5-4 Schematic of Stand- Alone Systems For Ac Loads 33
Figure 5-5 Schematic of Utility- Interactive Systems 33
Figure 5-6 Schematic of Hybrid Systems 34

ABSTRACT

The objective of this research is to develop a new type of hybrid concentrated Photovoltaic/Thermal (CPV/T) solar collector system that could partially fulfill a typical four people family's heat and electricity demands in many parts of the world.

A CPV/T system with a solar collector diameter of 6.18 m, 30 m^2 area along with 1.13 m radius, 4 m^2 and solar PV panel with spectral selection of radiation for the two devices is analyzed. The model developed assumes the use of new solar cell panels combined and concentration of solar energy dish that improves upon the efficiency of current photovoltaic thermal (PV/T) systems. With normal beam irradiance incident on the concentrated dish of about 1,000 W/m^2 under a clear sky around solar noon in New York city, the concentrated insolation to a notch filter with a transmissivity of 90 percent through which the radiation passes will increase up to 7,500 W/m^2 if the area of dish and PV receiver is 30 m^2 and 4 m^2 respectively. From the spectrally selected solar energy of wavelengths suitable for the PV receiver, about 22 percent of solar insolation (1,910 kWh/m^2 per year) will be transferred into electricity, and the rest of energy reflected into a cavity thermal receiver to be used as heat when the average normal beam insolation is 1,286 kWh/m^2 per year.

A detailed calculation for electrical efficiency based on the spectrally selected solar energy has been developed in this work. Calculations using Mathematica software indicate that electrical efficiency of non-concentrating system solar cells is about 55 percent using the Shockley-Queisser approach and 39 percent by the device-based method, and for the CPV/T system, the efficiency is 42 percent based on device-based method.

This CPV/T system could provide both electrical and thermal energy to a family of four with an average electrical consumption of about 16,900 kWh per year with about 2,781 kWh of electrical energy and 69 MMBtu of thermal energy per year.

CHAPTER 1. INTRODUCTION

1.1 Need for Renewable Energy

Fossil fuels are the main energy resources currently in the world. Data from Energy Information Administration (EIA), Figure 1-1, indicates that in 2007 the primary sources of energy consisted of petroleum and coal 36 and 27 percent, and with natural gas use at 23 percent, the total amounting to an 86 percent share for fossil fuels [6].

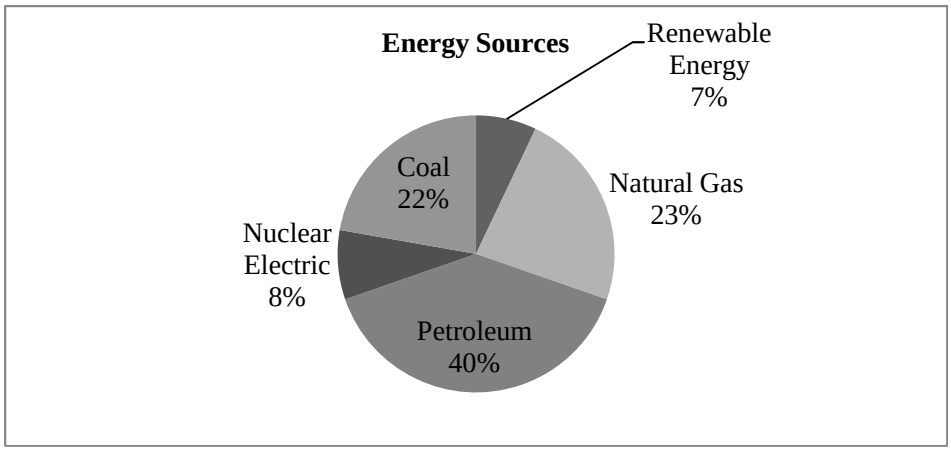

Figure 1-1 Percentage contributions of energy sources in 2007

Solar energy can be utilized in many ways: one way is solar thermal energy and the other is solar electrical energy. For solar thermal energy, we usually use different kinds of solar collectors that gather energy for fluid heating and/or space heating and cooling. For solar electrical energy, one could employ Si or other solar photovoltaic cells to transfer the solar energy into electricity directly. Thus, this process is called as photovoltaic (PV) and CPV when concentrated solar energy is used.

Since the energy crisis in the 1970s, many governments have supported research and applications of solar photovoltaic technology. In the past 30 years, most of countries set up solar energy plants and photovoltaic technology has been developed quickly.

As we all know, solar energy has become one of the best potentials for clean energy in the world. It has several advantages when compared with coal, oil and nuclear energy. Firstly, solar energy will not produce the fuel waste and harmful gases or pollute the

environment. Secondly, solar energy has no geographical and resource constraints and could be used safely and comfortably everywhere as long as there is sunlight. Therefore, research and application of solar energy is one of the aims of human energy development, though the penetration of solar energy into the energy mix has not made much progress, as shown in Figure 1-2 primarily due to cost considerations.

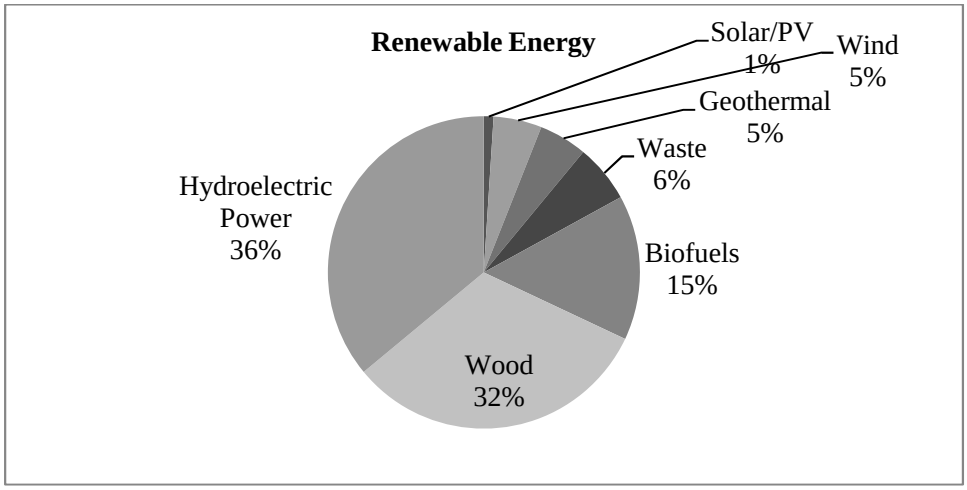

Figure 1-2 Percentage contributions of renewable energy in 2007

1.2 A Brief History about Solar Energy Utilization

As early as 1876, the British scientists Adams and Day discovered that the photo-generation of electrical current was when sunlight strikes Selenium, a semiconductor material. This is the first observation of Photovoltaic (PV) effect in solids. However, the photovoltaic effect is too small in Selenium and the conversion efficiency is only about 1 percent. The modern era of photovoltaics started in 1954 when researchers at Bell Labs in the U.S. accidentally discovered that p-n junction diodes generated a voltage when the room lights were on. In a year they had produced a 6 percent efficient Si p-n junction solar cell. In the same year, the group at Wright Patterson Air Force Base in the U.S. published results of a thin-film hetero-junction solar cell based on Cu_2S/CdS also having 6 percent efficiency, which turned out to be the fundamental research for thin film solar cell. Several years later, in 1959, Hoffman Electronics offered 10 percent efficient Si PV cells. By the early 1960s, the

design of cells for space use had stabilized, and over the next decade, this was their major application [2].

Because of the oil embargo in the Middle East War in 1973, the energy crisis related OPEC oil happened all over the world and then people realized the limitation and non-renewability of conventional energy. People realized the importance of renewable energy for the national security. Thus, every country began to develop the technology of solar energy and photovoltaics especially for large ground based photovoltaic research and applications.

An early development that helped many companies was to sell PV cells for industrial consumer-sized, small-scale power applications such as watches and solar-powered calculators. Another application was the rural electrification of remote off-grid villages in an attempt to help the roughly one-third of the world's citizens to gain access to a modest amount of electrical power, modern communications and lighting.

The present work looks into a small advance in solar energy where solar energy can be used for concentrated PV electrical generation as well as thermal energy collection.

The rest of this thesis consists of a brief review of literature, methodologies used in this work to evaluate the potential for spectrally demarked CPV/T solar systems, followed by a discussion of results generated in this effort followed by conclusions.

CHAPTER 2. BACKGROUND AND PAST WORK OF PV/T SYSTEMS

2.1 Solar Radiation

Though a mediocre star, our sun is our important star and is the center of our solar system; it supplies both sunlight and heat to us. Solar energy is a new type environmental friendly energy compared to fossil fuels. When the sunlight reaches the earth, most of it will have passed through the atmosphere and the radiation is called terrestrial radiation, the part that is not reflected to the outer space.

2.1.1 Principal Features of the Sun

The sun is a sphere of gas heated by a nuclear fusion reaction. The diameter of the sun is about 1.39×10^9m and the distance between the sun and the earth is 1.5×10^{11}m on average. The sun has an effective blackbody temperature at 5777K, where a blackbody is an idealized physical body that absorbs and emits all incident electromagnetic radiation. The effective blackbody temperature of 5777K means that a blackbody with the temperature of 5777K radiates the same amount of energy as does the sun. Temperature near the sun's center could be as high as 8×10^6 to 40×10^6K [3].

The sun is shown schematically in Figure 2-1. It consists of photo sphere, a region of convection along with the domain of fusion. Outside the photosphere is a more or less transparent solar atmosphere, observable during total solar eclipse or by instruments that occult the solar disk. The sun is essentially a sphere of gas heated by a nuclear fusion reaction in its center. The temperature and pressure inside the sun are extremely high that enables fusion reaction in the domain. As a result of Hydrogen fusion, Helium is generated. The mass of the Helium nucleus is less than that of the four nucleons (two protons and two neutrons), the mass (defect) having been 'lost' in the reaction and converted to energy. Approximately 6.2×10^{11}kg Hydrogen turns into Helium every second corresponding to the

mass defect of $4.3 \times 10^9 \text{kg/s}$ [1]. According to Einstein's theory of relativity, energy could be transferred from mass and mass-energy equivalence can be expressed as:

$$E = mc^2 \tag{2.1}$$

where m is mass, c is the speed of light in vacuum. Using this equation, we can find that 9×10^{16} joules energy can be obtained from 1 kilogram mass loss. Thus, the sun emits 3.8×10^{26} joules of radiative energy per second and the Earth receives approximately 170 million GW of power from the sun since Earth subtends very few steridians thus receiving only one over 22 hundred million of the total solar radiation [4].

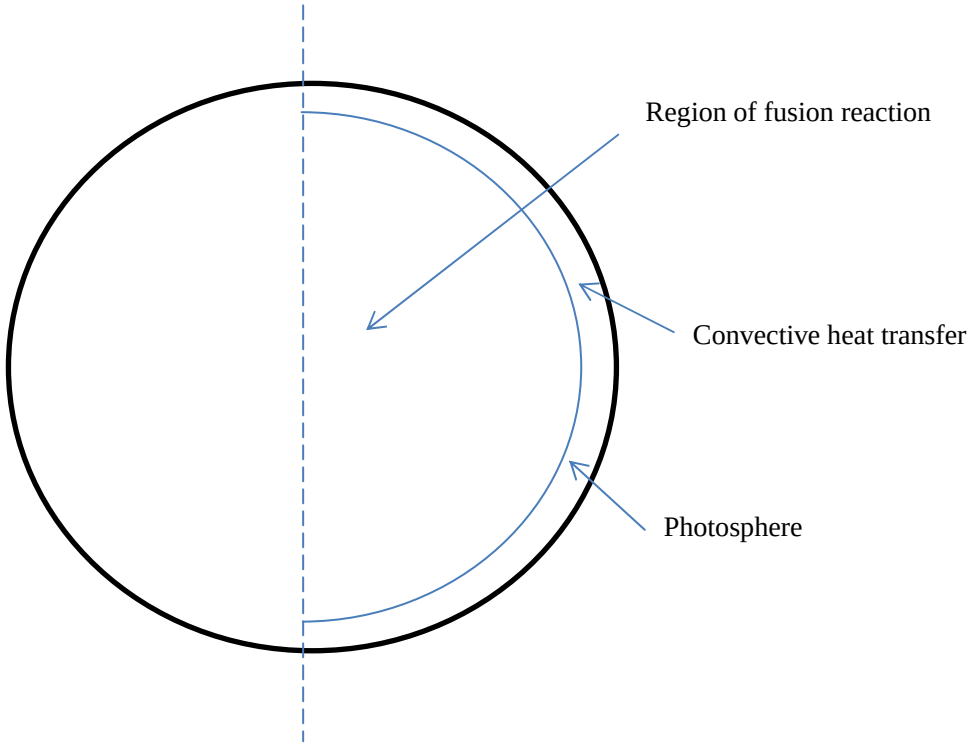

Figure2-1 Principal features of the sun

2.1.2 The Solar Constant

As is well known, the solar radiation varies with time and the earth-sun distance. We can calculate the radiant power per unit area perpendicular to the direction of the sun outside the earth's atmosphere but at the mean earth-sun distance though it is not easy to calculate the solar constant. However, we can use a weighted average of measurements made by equipment mounted on balloons, high-altitude aircraft, and spacecraft. Here, in this work we will use $1{,}353 \text{W/m}^2$ [3] as the solar constant.

2.1.3 Extraterrestrial and Terrestrial Solar Radiation

The spectral emissive power density of a blackbody is given by Planck's radiation law [5]:

$$E_{\lambda b}(\lambda, \mathrm{T}) = \frac{C_1}{\lambda^5\left[\exp\left(\frac{C_2}{\lambda T}\right)-1\right]} \tag{2.2}$$

where $C_1 = 3.7405 \times 10^8 \mathrm{W}\,\mu\mathrm{m}^4/\mathrm{m}^2$ and $C_2 = 1.43878 \times 10^4\ \mu\mathrm{mK}$ are called Planck's first and second radiation constants. $E_{\lambda b}$ is called the spectral emissive power density with units $\mathrm{W}/\mu\mathrm{m}\ \mathrm{m}^2$.

The ratio of the mass of atmosphere through which the beam radiation passes to the mass it would pass through if the sun were at the zenith can be described in terms of equation (2.3). Therefore, when the sun is directly overhead, the optical air mass is unity and the radiation is described as air mass one (AM1) radiation. When the sun is an angle θ to overhead, the air mass is given by

$$\text{Air Mass} = \frac{1}{cos\theta} \tag{2.3}$$

Comparing with the situation outside the earth's atmosphere, terrestrial sunlight varies greatly both in intensity and spectral composition. For example, when $\theta = 48.2^o$, the air mass (ratio) is 1.5, which is the most widely used terrestrial standard and the total peak power density content is $1{,}000\ \mathrm{W}/\mathrm{m}^2$. It is very common standard used when we try to find the efficiency of solar cells.

The spectral distribution of extraterrestrial radiation was measured from the data of spectral radiation on the ground at sea level and on mountains. However, these results are not accurate because of the differences in absorption, scattering, and reflection at various wavelengths by air molecules, water, CO_2 and O_3. It is a difficult measurement when the lower atmosphere air changes with cloud cover. But now, the availability of data with very high altitude aircraft, balloons, and spacecraft has permitted direct the measurements of spectral distribution and is indicated in Figure 2-2. Figure 2-2 also indicates various losses and absorption of solar radiation passes through our atmosphere.

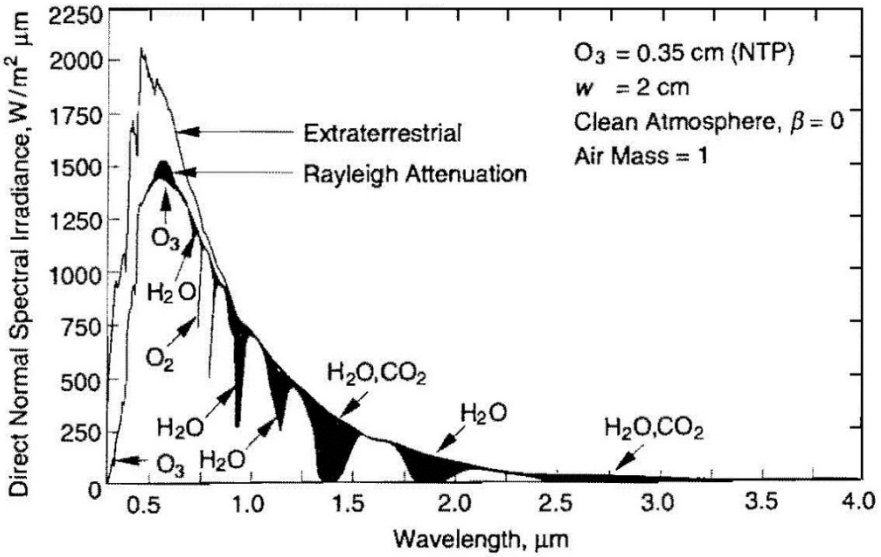

Figure 2-2 An example of the effects of Raleigh scattering and atmospheric absorption on the spectral distribution of beam irradiance [3].

From Figure 2-2, we can conclude that:

1. Nitrogen, Oxygen, and atmospheric molecules in the ionosphere will absorb gamma rays and X-rays.
2. Most of the Ultra Violet radiation will be absorbed by ozone
3. Visible radiation will mainly be scattered by atmospheric molecules, water vapor molecules, dust, and smog.
4. Near infrared will be absorbed by water vapor molecules selectively.

2.2 Semiconductors Physics and Solar Cells

A semiconductor is a material with electrical conductivity between a conductor and an insulator. From the chemical perspective, it is the crystal structure that makes semiconductors different from the conductors and insulators. Semiconductors have the capacity to absorb light and to deliver a portion of the energy of the absorbed photons transfer it to carriers of electrical current-electrons and holes.

2.2.1 Energy Band Structure

The difference in energy between electrons in the valence band and ones in the conduction band is called the band gap energy.

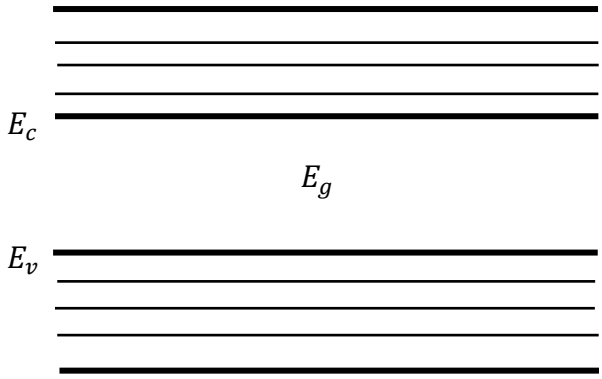

Figure 2-3 Energy band structure

Normally, the bands with lower energy are filled with electrons and we call them filled band, While, in the energy band diagram indicated in Figure 2-3, the bands with higher energy are usually empty and have no electrons occupied. Therefore, we call them conduction band. The electrons in the conduction bands, with an abundance of unoccupied energy states in the vicinity, can contribute to current flows.

The next-lower band is a filled band and the electrons in this band could be thermally excited into the conduction band. Therefore, we call it valence band.

The band gap energy of semiconductors is an important parameter that could affect the semiconductors' electrical and optical performance. Band gap energies for some typical materials used in photovoltaic cells are presented in Table 2.1.

Table 2.1 Representative photovoltaic material band gap energies [6]

Material	Band Gap Energy (eV)
Si, Silicon	1.11
CdTe, cadmium telluride	1.44
CdS, cadmium sulfide	2.42
$CuInSe_2$, copper indium diselenide	1.01
GaAs, gallium arsenide	1.40
GaP, gallium phosphide	2.24
InP, indium phosphide	1.27

2.2.2 Electrons and Holes

There are two kinds of carriers-electrons and holes in semiconductor materials and directional movement of electrons and holes results in the conduction of electricity. In the state of low temperature, the valence electrons are bound to surrounding nucleus and therefore, they could not move freely in the crystal. In other words, the valence band is fully filled while the conduction band is not occupied completely. However, as the temperature increases, or increase energy otherwise some electrons are excited into the conduction band, so states near the top of the valence band are empty. These empty states can conveniently be regarded as positively charged carriers of current called holes.

The equilibrium electron and hole concentrations are given by:

$$n_0 = N_C \exp\left(\frac{E_F - E_C}{kT}\right) \tag{2.4}$$

and

$$p_0 = N_V \exp\left(\frac{E_V - E_F}{kT}\right) \tag{2.5}$$

where the conduction band and valence band effective densities of state are given by:

$$N_C = 2\left(\frac{2\pi m_n^* kT}{h^2}\right)^{3/2} \tag{2.6}$$

and

$$N_V = 2\left(\frac{2\pi m_p^* kT}{h^2}\right)^{3/2} \tag{2.7}$$

Diode saturation current density can be expressed as:

$$J_0 = n_i^2\left(\frac{qD_n}{L_n N_A} + \frac{qD_p}{L_p N_D}\right) \tag{2.8}$$

where n_i is the intrinsic semiconductor concentration,

$$n_i^2 = N_C N_V \exp\left(-\frac{E_g}{kT}\right) \tag{2.9}$$

and for silicon, $n_i = 1.06 \times 10^{10} cm^{-3}$ [7]. D_p and D_n are the hole and electron diffusion coefficients, respectively. N_D and N_A are the total densities of donors and acceptors, respectively and L_n and L_p are the electron and hole diffusion lengths.

$$L_n = \sqrt{D_n \tau_n} \tag{2.10}$$

The above equations are useful in calculating the saturation current density of solar cells when the specific semiconductor parameters are known.

2.2.3 P-N Junction Diode Electrostatics

PN-junction is the core of the most semiconductor devices and is the backbone of the integrated circuit (IC) as well. Also, it is the main unit of the solar cells.

Where an n-type semiconductor comes into contact with a p-type semiconductor, a PN-junction is formed, as shown in Figure 2-4.

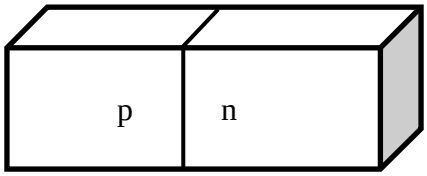

Figure 2-4 P-N junction model

In thermal equilibrium, the diffusion and drift currents for each carrier type exactly balance, so there is no net current flow. The transition region between the n-type and the p-type semiconductors is called the space-charge region. It is also called the depletion region, since it is effectively depleted of both holes and electrons. The electrostatic potential difference resulting from the junction formation is called the built-in voltage, V_{bi}[2].

The electrostatics of this situation is given by Poisson's equation:

$$\nabla^2 \emptyset = \frac{q}{\varepsilon}(n_0 - p_0 + N_A^- - N_D^+) \tag{2.11}$$

where $\emptyset$ is the electrostatic potential, q is magnitude of the electron charge, ε is the electric permittivity of the semiconductor, p_0 is the equilibrium hole concentration, n_0 is the equilibrium electron concentration, N_A^- is the ionized acceptor concentration, and N_D^+ is the ionized donor concentration.

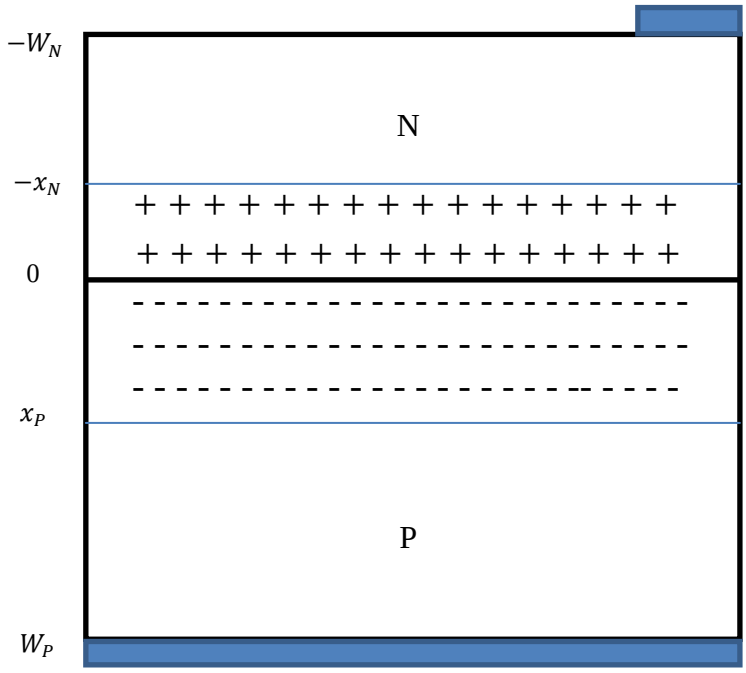

Figure 2-5 Simple solar cell structure [2]

Here is an assumption. Within the depletion region, we could ignore the p_0 and n_0 as they are so small compared to $|N_A^- - N_D^+|$. Thus, the Poisson's equation yields:

$\nabla^2\emptyset = -\frac{q}{\varepsilon}N_D$, for $-x_N < x \leq 0$

and

$\nabla^2\emptyset = \frac{q}{\varepsilon}N_A$, for $0 < x \leq x_P$

Outside the depletion region, charge neutrality is assumed and

$\nabla^2\emptyset = 0$, for $x \leq -x_N$ and $x \geq x_P$

If we assume that $\emptyset(x_P) = 0$, we can solve the Poisson's equation step by step:

For $x \geq x_P$, $\emptyset(x) = 0$

For $x \leq -x_N$, $\emptyset(x) = V_{bi}$

For $-x_N < x \leq 0$, $\emptyset(x) = V_{bi} - \frac{qN_D}{2\varepsilon}(x + x_N)^2$

For $0 \leq x < x_P$, $\emptyset(x) = \frac{qN_A}{2\varepsilon}(x - x_P)^2$

The electrostatic potential has to be continuous at *x*=0, that is:

$$V_{bi} - \frac{qN_D}{2\varepsilon}(x_N)^2 = \frac{qN_A}{2\varepsilon}(x_P)^2 \qquad (2.12)$$

Also, the electric field should be continuous at the interface.

$$x_N N_D = x_P N_A \tag{2.13}$$

In thermal equilibrium, the net hole and electrons currents have to equal zero. For the hole current density is:

$$\overrightarrow{J_p} = q\mu_p p_0 \vec{E} - qD_p \nabla p = 0 \tag{2.14}$$

From the Einstein relationship,

$$\mathrm{D} = \frac{\mu kT}{q} \tag{2.15}$$

The electric field yields:

$$\vec{E} = \frac{kT}{q}\frac{1}{p_0}\frac{dp_0}{dx} \tag{2.16}$$

Then, we could calculate the local voltage build up:

$$V_{bi} = \int_{-x_N}^{x_P} \vec{E}\,dx = \int_{-x_N}^{x_P} \frac{kT}{q}\frac{1}{p_0}\frac{dp_0}{dx}dx = \frac{kT}{q}\int_{p_0(-x_N)}^{p_0(x_P)} \frac{dp_0}{p_0} = \frac{kT}{q}\ln\left[\frac{p_0(x_P)}{p_0(-x_N)}\right]$$

If we assume non-degeneracy in the semiconductor, we have $p_0(x_P) = N_A$ and $p_0(-x_N) = \frac{n_i^2}{N_D}$.

Therefore,

$$V_{bi} = \frac{kT}{q}\ln\left[\frac{N_A N_D}{n_i^2}\right] \tag{2.18}$$

2.2.4 Solar Cell I-V Characteristics

The basic solar cell structure has now been established as we can see from Figure 2-5. Typically, the more heavily doped quasi-neutral region is called the emitter and the more lightly doped region is called the base. The emitter region is very thin and most of the light absorption occurs in the base.

From the pn-junction diode electrostatics, we know that the depletion region does not have many free or mobile charges. Therefore, the total current is determined by the minority carrier current densities.

A general equation for the current density produced from a solar cell is [15]

$$J = J_{sc} - J_{o1}\left(e^{\frac{qv}{kT}} - 1\right) - J_{o2}\left(e^{\frac{qv}{2kT}} - 1\right) \quad (2.19)$$

where J_{sc} is the short-circuit current density and is the sum of the contribution from each of the three regions: the n-type region, the depletion region, and the p-type region.J_{o1} is the dark saturation current density due to recombination in the quasi-neutral regions. J_{o2} is the dark saturation current density due to recombination in the space-charge region (the depletion region). A simple solar cell circuit model is indicated in Figure 2-6.

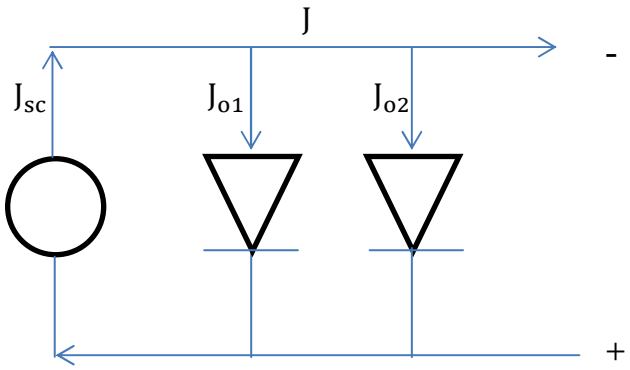

Figure 2-6 Simple solar cell circuit model

At open circuit ($I = 0$), all the light-generated current, I_{sc} is flowing through diode 1, so the open-circuit voltage can be written as

$$0 = J_{sc} - J_{o1}\left(e^{\frac{qv}{kT}} - 1\right)$$

$$V_{oc} = \frac{kT}{q}\ln\frac{J_{sc}+J_{o1}}{J_{o1}} \approx \frac{kT}{q}\ln\frac{J_{sc}}{J_{o1}} \quad (2.20)$$

Where $J_{sc} \gg J_{o1}$ in most situations, and J_{o1} can be obtained from equation 2.8.

2.3 Introduction of Current Hybrid Solar System

A hybrid solar system is considered in this section. An extensive amount of research on PV-thermal collectors has been carried out over the past 25 years. A hybrid photovoltaic-thermal (PV/T) solar energy system consists of a normal PV panel at the back of which a heat exchanger with fins is embedded, as shown in Figure 2-7. The advantage of this type of

system is that the PV panel operates at a lower temperature, thus more efficiently, and also hot water is produced at the same time along with electricity

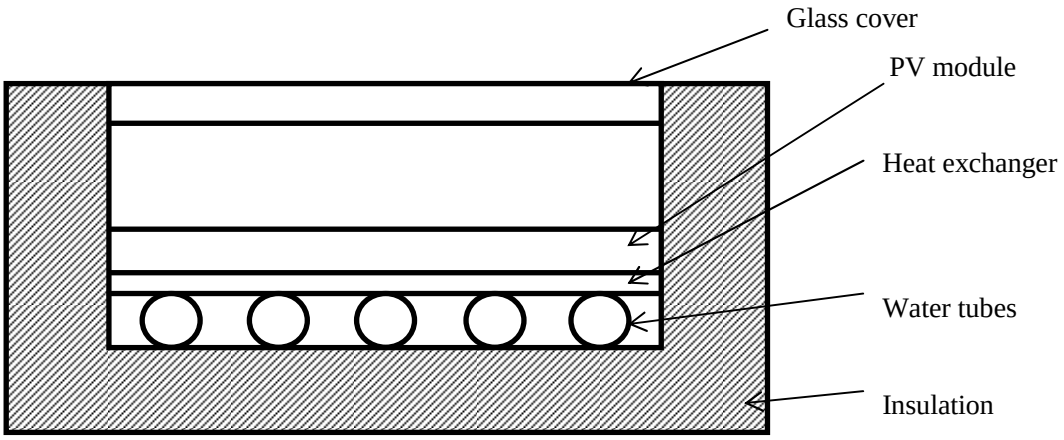

Figure 2-7 A hybrid PV/T Collector [8]

A steady state thermal efficiency η_{th} of the hybrid PV/T systems can be calculated by the relation:

$$\eta_{\mathrm{th}} = \frac{Q_u}{\mathrm{AI_b}} \tag{2.21}$$

where, A is collector area of this system and $\mathrm{I_b}$ is incoming solar insolation. The removed from the system $\mathrm{Q_u}$ can be written in terms of $\dot{m}$ the fluid mass flow rate, $\mathrm{T_0}$ and $\mathrm{T_i}$ outlet and inlet fluid temperature respectively and $\mathrm{c_p}$ is the fluid specific heat.

The PV module electrical efficiency η_{el} for PV cells of area $\mathrm{A_c}$ can be written using the following relation:

$$\eta_{\mathrm{el}} = \frac{\mathrm{P_c}}{\mathrm{A_c I_b}} \tag{2.22}$$

where, $\mathrm{P_c}$ is the output power of PV cells.

The steady state thermal efficiency could be calculated by using Hottel's approach [9].

A conventional flat plate solar collector is shown in Figure 2-8 and its mathematical model is indicated in Figure 2-9.

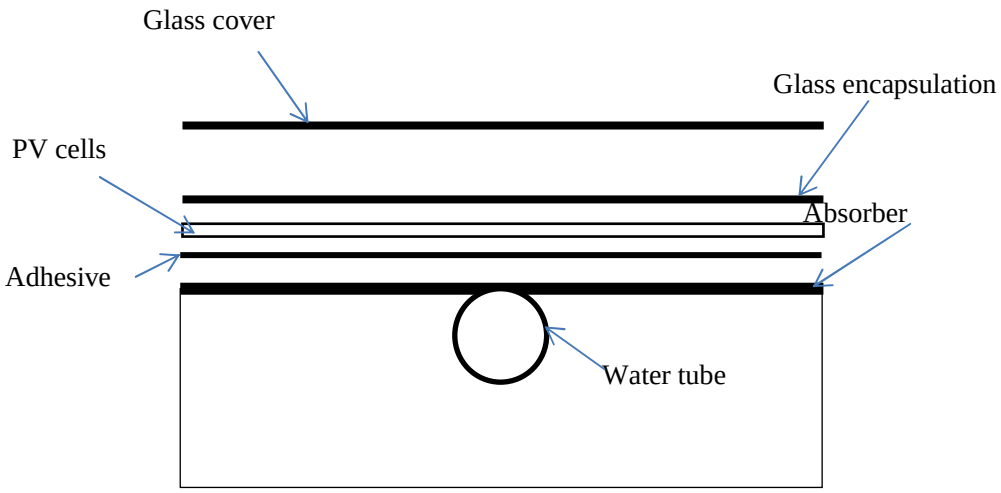

Figure 2-8 Typical sheet and tube PV/T collector

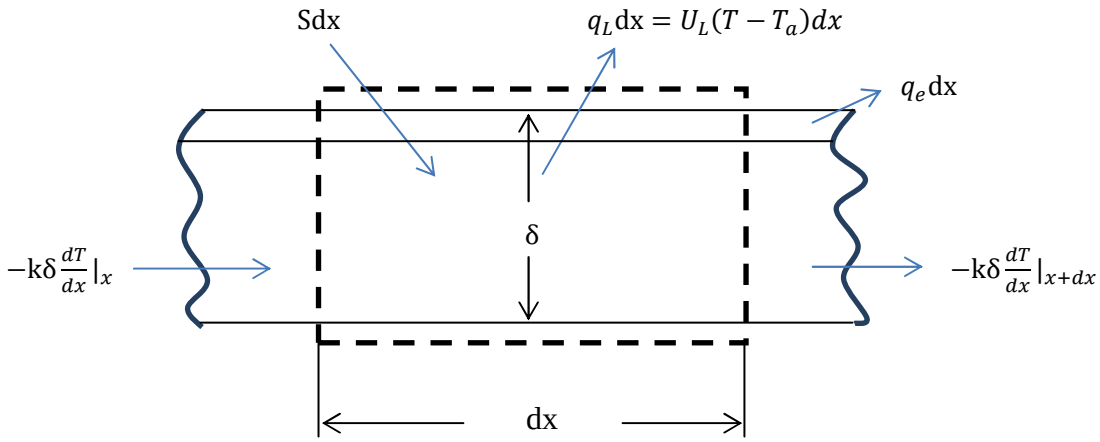

Figure 2-9 Energy balance model for PV/T collector [3]

From Figure 2-9, the steady-state energy balance of fluid temperature distribution on this element yields:

$$Sdx - U_L(T - T_a)dx - q_e dx + \left(-k\delta \frac{dT}{dx}|_x\right) - \left(-k\delta \frac{dT}{dx}|_{x+dx}\right) = 0 \qquad (2.23)$$

Where, S is the absorbed solar energy, q_e is the local unit area electrical output of collector, q_L is local unit area thermal loss rate from collector. T_a is ambient temperature.

Based on finite difference theory, we know that:

$$\frac{dT}{dx}|_{x+dx} = \frac{dT}{dx}|_x + dx\frac{d^2T}{dx^2}|_x + \cdots$$

Therefore, equation 2.23 can be expressed as:

$$\frac{d^2T}{dx^2} = \frac{1}{k\delta}[U_L(T - T_a) - S + q_e] \tag{2.24}$$

This second- order differential equation was analyzed by Duffie and Beckman [3].

Here, the results of this equation are presented.

The useful collected heat Q_u is given by:

$$Q_u = A_c F_R[S - U_L(T_i - T_a)] \tag{2.25}$$

where,

$$F_R = \frac{\dot{m}C_p}{A_c U_L}\left[1 - e^{-\frac{A_c U_L F'}{\dot{m}C_p}}\right]$$

$$F' = \frac{\frac{1}{U_L}}{W\left[\frac{1}{U_L[D_0 + (W - D_0)F]} + \frac{1}{C_b} + \frac{1}{\pi D_i h_{fi}}\right]}$$

$$F = \frac{\tanh(x)}{x}$$

and

$$x = \sqrt{\frac{U_L}{k\delta}}\left(\frac{W - D_0}{2}\right)$$

where W is the tube spacing and D_0 is the outside tube diameter.

Therefore, when all the parameters are known, we can finally calculate the thermal efficiency η_{th} of the hybrid PV/T system.

For the calculation of PV module electrical efficiency, Zondag et al. 2003 [8] expressed the equation as:

$$\eta_{el} = \eta_0[1 - 0.0045(T - 25^0C)] \tag{2.26}$$

where, $\eta_0$is PV electrical efficiency when ambient temperature is 25^0C and we have to assume that the cell efficiency decrease linearly with absorber temperature.

The solution of Duffie and Beckman is widely investigated in flat-plate solar heat collectors and it is also a good method for the thermal analysis of a hybrid photovoltaic/thermal system. The efficiency of solar cells is temperature dependent with decreasing efficiency as the temperature increases as shown in equation 2.26. For example,

crystalline silicon solar cells will have a decrease in efficiency of 15 percent when the temperature increases 30 K. However, it may not be worth collecting energy from the back of a PV system in order to achieve a better PV efficiency. First of all, although there is about 64 percent of solar energy dissipated as heat in solar cells [19], we cannot collect it completely because natural convection is used between cells and air. Secondly, collecting energy from the back of the PV is too small to heat the water needed above 40 ^{o}C. Therefore use of a notch filter so that the cells just absorb the useful spectrum and the rest of solar insolation be collected for thermal use. That is an important idea developed for a new type of CPV/T system.

CHAPTER 3. A NEW TYPE OF CPV/T SYSTEM

In this section, a new type of concentrating photovoltaic/thermal (CPV/T) device is described that uses concentrated PV as well as thermal energy collection as shown in Figure 3-1.

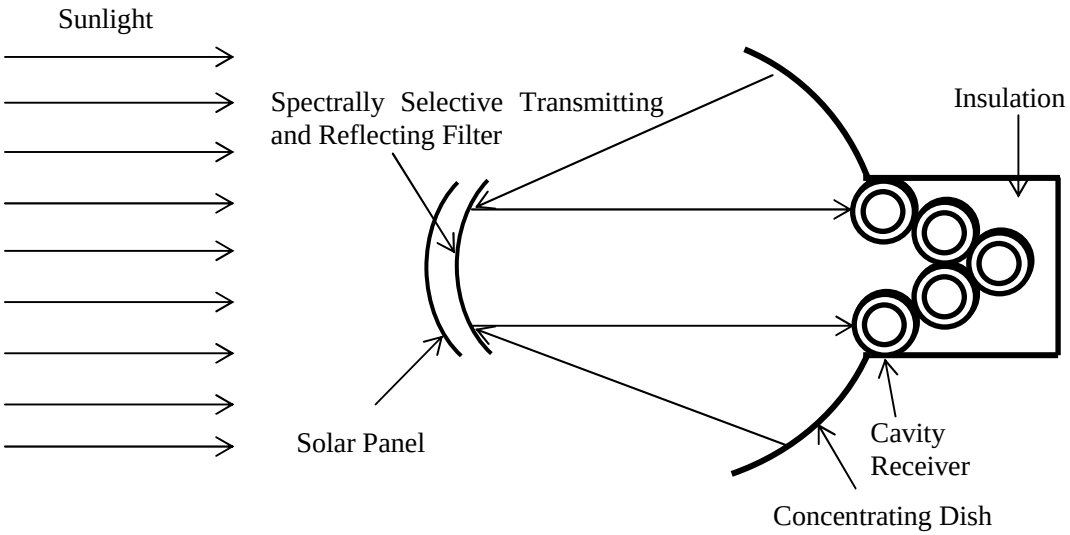

Figure 3-1 A new type hybrid solar system

The device uses a concentrator as well as a cavity receiver. The Cassegraine reflector reflects selected wavelengths of lights in appropriate for PV (too short or too long wave lengths). This is achieved with a notch filter. The CPV cells mounted at the Cassegraine behind the filter are designed to receive only the photons that match the PV band gap. All solar radiation below or above the desired band gap is reflected into the cavity receiver for thermal energy collection.

3.1 Performance of the notch Filter

Spectral energy control is a major factor in attaining high efficiency for this hybrid PV/T energy converter. Placing an optical filter between the parabolic concentrator and PV array is one method for spectral control and is used in this current model.

In order for achieving high system efficiency, the filter must have low absorptance. It must have large transmittance in the useful photon energy region. For example, the photon energy, E closed to the PV cell band gap energy, E_g, or $\lambda < \lambda_g = \frac{hc_o}{E_g}$ should pass through the filter to PV and all other energy reflected outside this region ($E > E_g$ or $E < E_g$).

The performance of a filter will be determined by the transmittance,τ_f, reflectance, ρ_f, and absorptance, α_f, as well as a filter efficiency, η_f.

3.2 Performance of Parabolic Concentrators

The absorbed radiation for concentrating collectors:

The absorbed energy for the useful aperture area of the collector is then

$$S = I_{b,a}\rho(\gamma\alpha)_n K_{\gamma\alpha} \tag{3.1}$$

where $I_{b,a}$ is the effective incident radiation measured on the plane of the aperture only beam radiation; ρ is the specular reflectance of the concentrator; γ is defined as the fraction of the reflected radiation, and α is defined as the fraction of the absorbed radiation [10]. The maximum concentration ratio for a three-dimensional concentrator system is, for spherical receivers:

$$C_{max} = \frac{sin^2\phi_r}{4sin^2\left(0.267+\frac{\delta}{2}\right)} - 1 \tag{3.2}$$

where ϕ_r is the rim angle.

Concentration ratio:

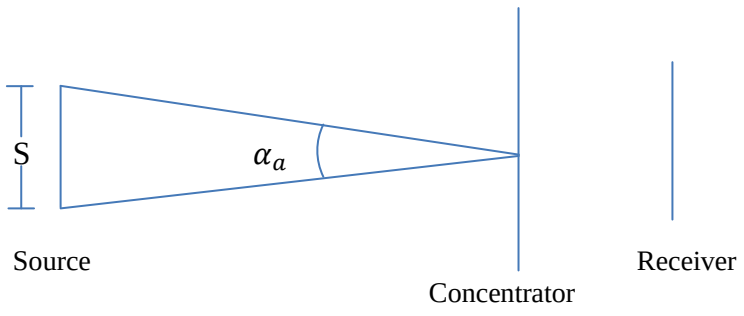

Figure 3-2 Schematic of concentrating collector

Concentration ratio can also be referred to an area concentration ratio, defining the ratio of the area of aperture to the area of the receiver.

$$\mathrm{C} = \frac{A_a}{A_r} \tag{3.3}$$

The 2-D concentrator only collects solar energy with some angle limitation. We call this angle received angle α_a. For the 2-D concentrator, the maximum concentration ratio is

$$C_{max,2D} = \frac{1}{\sin\left(\frac{\alpha_a}{2}\right)} \tag{3.4}$$

A flat collector can receive solar energy within the range of 180℃

For the observer on Earth, $\alpha_a \approx 0.5$℃

For the 3-D concentrator, the maximum concentration ratio is

$$C_{max,3D} = \frac{1}{sin^2\left(\frac{\alpha_a}{2}\right)} \tag{3.5}$$

We shall use parabolic solar concentrator dish with two-axis tracking system in the present model. Parabolic dish collector will reflect the parallel rays into the focus point. Consider the parabolic mirror shown in Figure 3-2. Assuming that the specular reflectance of the parabolic dish (ρ) is 0.86, and the fraction of the absorbed radiation (α) is 0.9, and the area of the dish (A_d) is $30\mathrm{m}^2$, and the area of solar panel (A_c) is $4\mathrm{m}^2$, we can calculate how much radiation incident on the panel when the local normal beam irradiance (I_b) is 1,000 W/m^2 in New York City.

$$\mathrm{I} = (\rho\alpha) I_b (A_d - A_c) = 20{,}124\mathrm{W}$$

Therefore, the local flux concentration ratio (C) is

$$\mathrm{C} = \frac{20{,}124 \dfrac{\mathrm{W/m^2}}{4\ \mathrm{m^2}}}{1{,}000\ \mathrm{W/m^2}} = 5$$

3.2 Cavity Receiver

For the collection of most of sunlight reflected from the filter, we need a receiver to collect this energy as heat. Therefore, the thermal part of this model is developed.

For many solar systems water is the ideal material in which to store usable heat at low temperatures. Because the shape of cavity is circular, the performance of storage receiver should have the following appearance as shown in Figure 3-3.

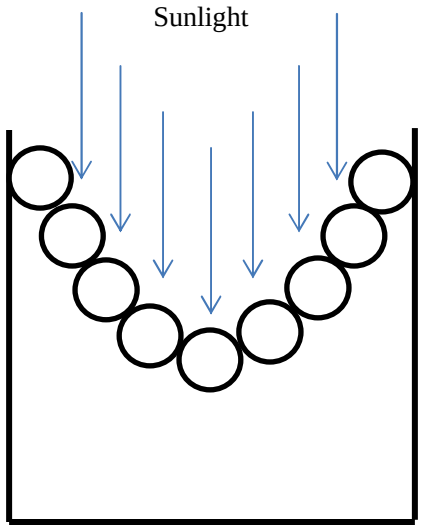

Figure 3-3 Schematic of cavity receiver

So how much energy is collected in the receiver and how much in the CPV system. What is the conclusion for this section? Write the material added in a different color so that I will concentrate on ONLY the newly added material. I will not have to read all the pages again.

The average beam irradiation is 1,286 kWh/m^2 per year in New York City. Of this 6,620 kWh energy can be absorbed by the CPV system with an output of electricity of 2,781 kWh, while the thermal receiver collects the rest of 20,140 kWh energy. In a word, with the help of concentrating dish and notch filter, we can obtain more electrical and thermal energy.

CHAPTER 4. EVAULATION OF CPV/T DISH

To analyze the CPV/T dish of interest, several assumptions are made and each is listed below as part of the analysis:

4.1 Solar Radiation Estimation in New York City

While the calculations and procedure used here are applicable for anywhere on the plant, New York City is assumed to be the location. The extraterrestrial radiation $\overline{H}$ on a horizontal surface on clear-day radiation is [3]:

$$\overline{H} = \overline{H_o}\left(a + b\frac{n}{N}\right) = \overline{H_o}\ \overline{K_t} \tag{4.1}$$

where $\overline{H}$ is the monthly average daily total radiation on horizontal surface. $\overline{H_o}$ is the monthly average daily extraterrestrial radiation on horizontal surface and can be expressed like as:

$$H_o = \frac{24\times3600G_{sc}}{\pi}\left(1 + 0.033cos\frac{360n}{365}\right)\times\left(cos\phi cos\delta sin\omega_s + \frac{\pi\omega_s}{180}sin\phi sin\delta\right) \tag{4.2}$$

where G_{sc} is the solar constant and here we will use $G_{sc} = 1353\ W/m^2$and n is the day of the year; ω_s is the sunset hour angle; ϕ is solar azimuth angle; δ is the declination. a and b are constants depending on location. $\frac{n}{N}$ is monthly average daily hours of bright sunshine over the maximum possible daily hours of bright sunshine. K_t is the day's clearness index. Obviously, a, b, $\frac{n}{N}$ and K_t depend on location.

In order to estimate the monthly average daily radiation in the clear-sky (sunny days), Jordan introduced an empirical formula that applies to everywhere and is only related to the solar azimuth angle ϕ:

$$G = A[C + cos\phi]\exp\left(-\frac{B}{cos\phi}\right) \tag{4.3}$$

where A, B and C are empirical constants determined by atmosphere.

There are not many good methods to calculate the diffuse and beam radiation. A broader database and improved understanding of the data will probably lead to improved method.

With the help of PVSYST, solar energy simulation software, one could easily know the solar radiation information for most cities. Here, for New York City and the following data tables give global, beam and diffuse radiation by the month.

Table 4.1 Monthly global, beam and diffuse irradiance in New York City

Month	Global on horizontal plane (W/m^2)	Beam on horizontal plane (W/m^2)	Diffuse on horizontal plane (W/m^2)
1	77.2	37.2	39.9
2	117.3	62.6	54.6
3	156.6	79.3	77.3
4	206.4	108.6	97.8
5	233.7	112.8	121.0
6	262.5	127.6	134.9
7	253.1	123.7	129.4
8	225.1	109.1	116.0
9	182.4	93.8	88.6
10	135.2	70.4	64.8
11	79.4	31.2	48.2
12	68.7	30.1	38.6
Year	166.7	82.3	84.4

4.2 Efficiency Calculation for CPV/T Dish

The theoretical efficiency of the solar cell is calculated here. The spectral energy is split into two parts; one has the wavelength between 800nm and 1120nm matching band gap, and the other is the rest of it, as shown in Figure 4.1. The PV efficiency with the incident sunlight with wavelength between 800nm and 1120nm needs to be defined.

Two approaches have been taken to calculate the limiting performance of silicon solar cells.

In the Shockley-Queisser approach (detailed balance method) the efficiency is calculated as a function of band gap for hypothetical semiconductors with step function optical absorptions and radiative recombination only.

The step function considered is:

$$I_0 = q\pi \int_0^\infty \frac{2}{h^3}\frac{E^2}{c^2} \exp\left(-\frac{E}{kT}\right) \alpha(E) dE \qquad (4.4)$$

with $\alpha(E)$ as the absorptance of the semiconductor ($0 < \alpha(E) < 1$). The absorbance assumed to be zero for $E < E_g$ and unity for $E > E_g$ [11].

The weak point of this method is that first, in the real materials the absorbance will always be a continuous function rather than a step function. Secondly, this approach neglects Auger recombination, which is as important a loss mechanism as radiative recombination [17].

First, let us calculate the PV efficiency without the effect of a spectral filter.

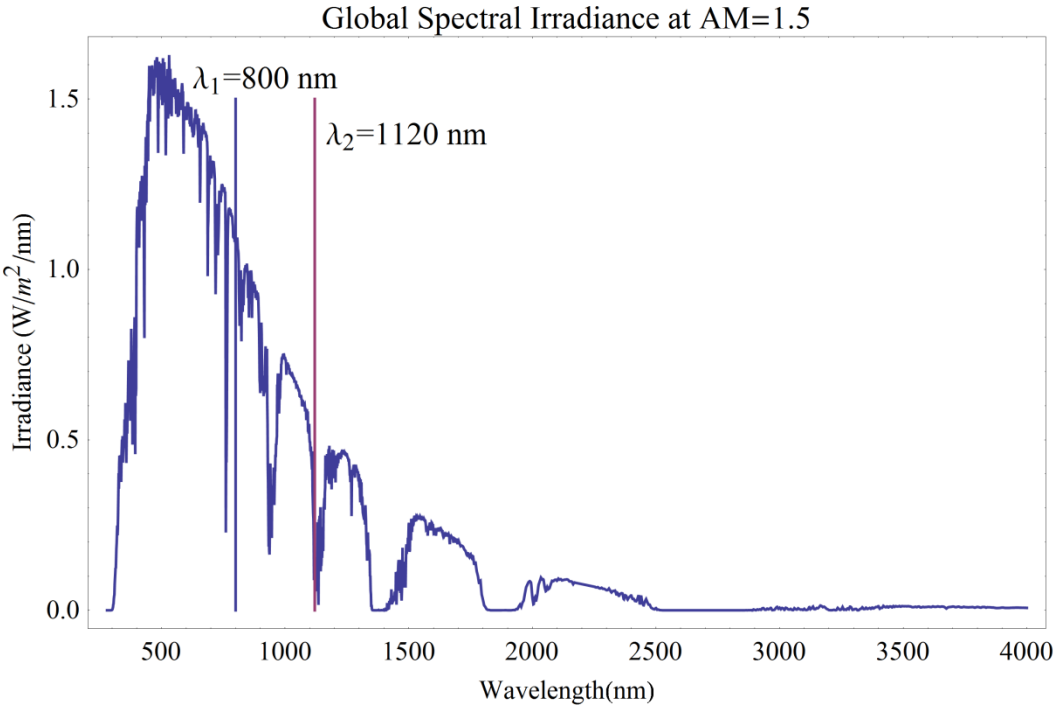

Figure 4-1 Global spectral irraidance at AM=1.5

NREL's data for the solar spectrum (AM 1.5) as shown in Figure 4-1 is used for these calculations and with the help of Mathematica software the efficiency is calculated.

Using Mathematica the procedure using the Shockley-Queisser limit (detailed balanced method) is:

Step1: Determining the solar spectrum

Step2: Calculate the incident solar power (integrated)

Step3: Calculate the numbers of photons above band gap

Step4: Calculate the radiative recombination rate

Step5: Determine the open-circuit voltage and short-circuit current density, the power and

Step6: Determine the maximum efficiency

Some of the data for the above calculations followed by the calculational procedure used are presented below.

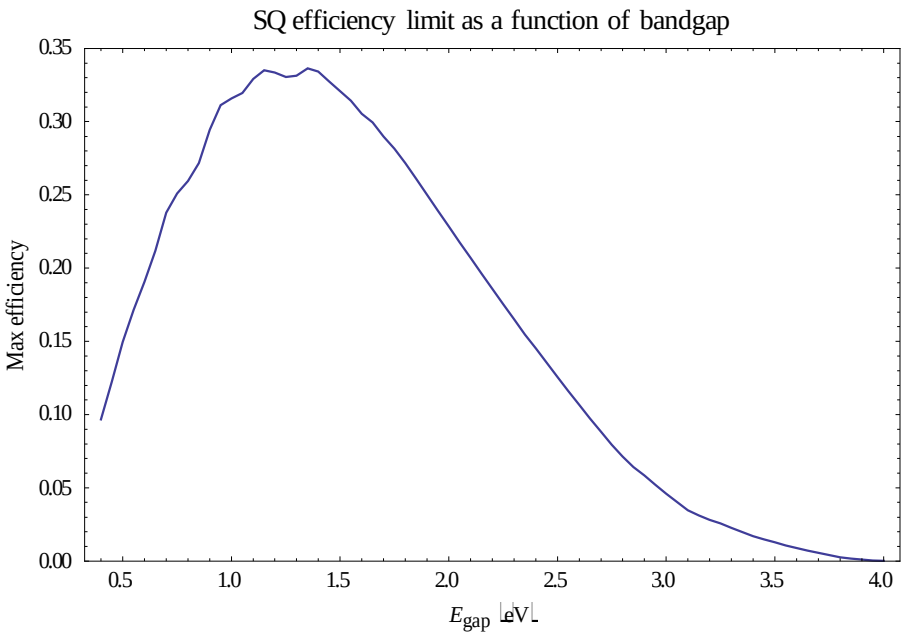

Figure 4-2 Shockley- Queisser efficiency limit as a function of bandgap

Then, we can get the reverse saturation current density:

$$J_0 = 1.0745 \times 10^{-8} A/m^2$$

When using the Shockley-Queisser Approach, we get the reverse saturation current density:

$$J_0' = 8.23066 \times 10^{-13} A/m^2$$

As we can see, $J_0$is larger than J_0'. The reason is that we only take the radiative recombination into account other than other recombination.

For SQ approach,

$$J' = 438.11 - 8.23066 \times 10^{-13} \exp(38.6817V) \quad (4.5)$$

and the open-circuit voltage will be

$$V_{oc}' = 0.8766 \text{ volt}$$

Then, the maximum efficiency based on all wavelengths:

$$\eta_{max}{}' = 0.334$$

For the device-based approach,

$$J = 438.11 - 1.0745 \times 10^{-8} \exp(38.6817V) \quad (4.6)$$

That will change the open-circuit voltage to:

$$V_{oc} = 0.6316 \text{ volt}$$

Therefore, the maximum efficiency for the device-based approach will be

$$\eta_{max} = 24.1\%$$

Not surprisingly, Figure 4-3 indicates that the cell has maximum efficiency when the band gap of semiconductor is 1.14 eV.

Now we calculate the maximum efficiency of silicon solar cell with filter (with incident solar radiation between 800 - 1,100 nm). The selective filter used for the photons transmitting photons with energy between 1.12 eV and 1.55 eV can pass through and reflect the rest. The methods described earlier are used to evaluate the efficiency.

SQ Approach:

The spectrum distribution with the photon wavelength from 800 nm to 1,120 nm is displayed below:

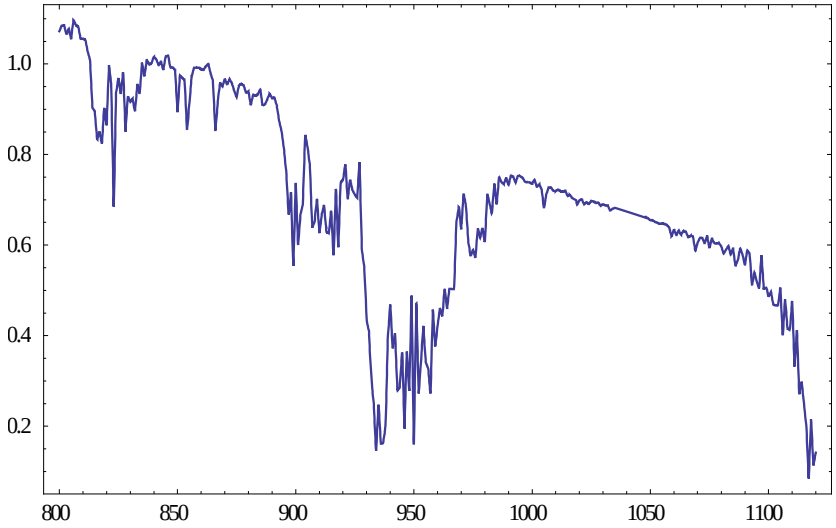

Figure 4-3 Spectrum distribution with the photon wavelength between 800nm and 1,120nm

Energy input (solar irradiation) for photon wavelength from 800 nm to 1,120 nm onto PV cells:

$$\mathrm{P_{in}} = 222.52\ \mathrm{W/m^2}$$

Calculate the number of incident photons (Energy from 1.12eV to 1.55eV):

$$Nphoton = 1.032 \times 10^{21}\ cm^{-2}sec^{-1}$$

Then the short-circuit current density will be:

$$J_{sc} = e\ Nphoton = 16.54\ \mathrm{mA}/cm^2,$$

and the radiative recombination rate will be:

$$RR = 5.14 \times 10^{6} m^{-2} sec^{-1}$$

The reverse saturation current density:

$$J_0 = e\, RR = 8.23 \times 10^{-13} \mathrm{A}/m^2,$$

and the Ampere-Voltage characteristic formula:

$$J = 165.4 - 8.23 \times 10^{-13} \exp(38.68\, V) \tag{4.7}$$

For the above, the open-circuit voltage will be:

$$V_{oc} = 0.8514 \text{ volt}$$

For these conditions, the maximum efficiency:

$$\eta_{max} = \frac{FF J_{sc} V_{oc}}{P_{in}} = 0.55$$

which is almost twice the value of the prior calculated efficiency for the PV.

Device-based Method:

Following the above procedure, the device based reverse saturation current density is:

$$J_0{}' = 1.0745 \times 10^{-8} A/m^2$$

The Ampere-Voltage characteristic formula for the saturation current is:

$$J = 165.4 - 1.0745 \times 10^{-8} \exp(38.682\, V) \tag{4.8}$$

and the open-circuit voltage is (I-V characteristic curve indicated in Figure 4.4):

$$V_{oc} = 0.6064 \text{ volt}$$

The maximum efficiency for these conditions will be:

$$\eta_{max} = 0.39$$

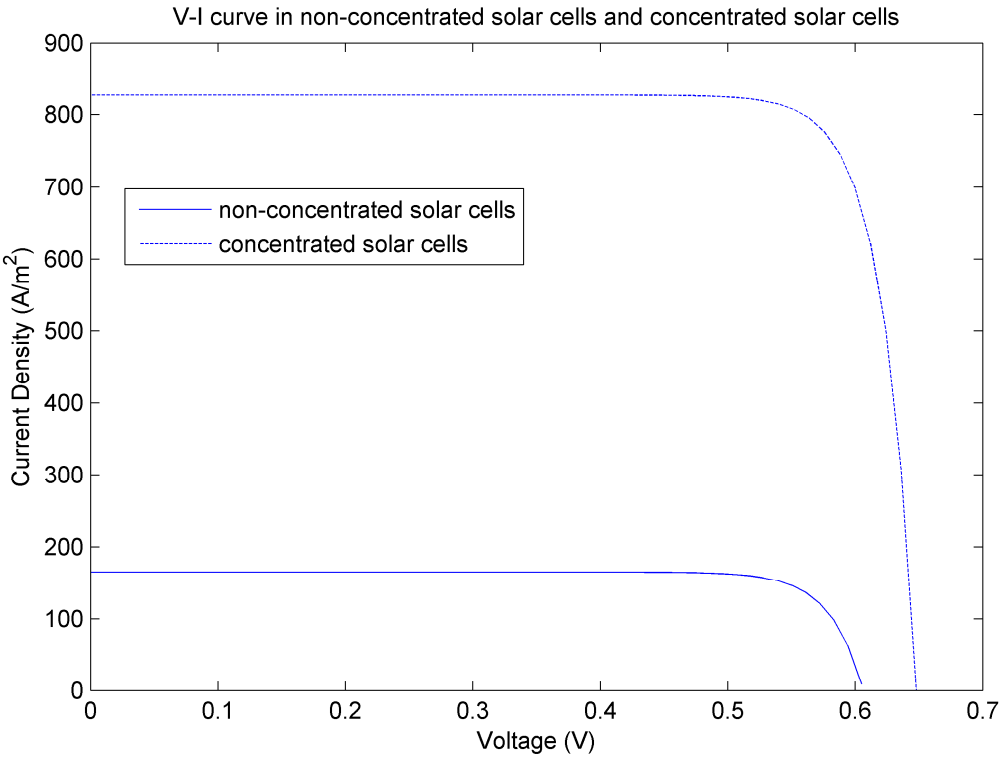

Figure 4-4 Current-Voltage characteristic for spectrally selective concentrated photovoltaic (CPV) and non-concentrated solar cells

For the efficiency of concentrating solar cells, Calculation of efficiency for concentrating solar cells is done as follow:

The local flux concentration ratio (x) is about 5 as presented in chapter 4. Thus the short-circuit current density at that concentration is:

$$J_{sc}^{xsuns} = xJ_{sc}^{1sun} = 5 \times 165.4\ A/m^2 = 827\ A/m^2$$

The open-circuit voltage is:

$$V_{oc}^{xsuns} = V_{oc}^{1sun} + \frac{kT}{q} lnx = 0.6064 + 0.0416 = 0.648\ \text{V}$$

Therefore, the efficiency of concentrating solar cells (I-V characteristic curve also indicated in Figure 4.4) can be expressed as:

$$\eta_c = \frac{FF\ V_{oc}^{xsuns}\ J_{sc}^{xsuns}}{x\ P_{in}} = 0.42$$

In summary, the peak efficiency of the CPV in the CPV/T system is 42 percent when the local solar irradiance is 1,000 W/m^2. Because of the higher electrical efficiency of the CPV system in the CPV/T system, we can collect more electricity in this system.

CHAPTER 5. ENERGY ANALYSIS OF THE CPV/T DISH

5.1 Photovoltaic System Configurations

Generally speaking, photovoltaic systems can be classified as 'Stand-Alone' systems, 'Utility-Interactive' system and Hybrid systems [4]. Stand-alone systems include some types of PV systems that supply power to off-grid electrical loads. Therefore, stand-alone systems are most popular for small to intermediated size electrical loads such as in remote, off grid areas. Stand-alone systems can include direct-coupled systems, self-regulated systems, charge-controlled systems and Stand-Alone Systems for AC loads. The differences among these systems are mainly their components.

a) Direct-Coupled Systems

These systems are usually used in small scale applications and consist of only an array and a DC load. The disadvantage of this system is the load must be able to operate over a range of power levels for different insolation.

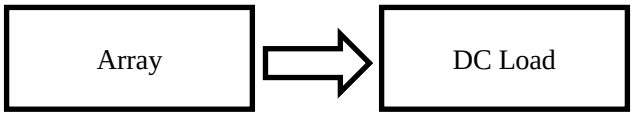

Figure 5-1 Schematic of Direct Couple Systems

b) Self-Regulated Systems

Most stand- alone systems need energy storage in case of lower solar insolation and per today's state-of the- art, batteries are the most common choice. This system is the same as direct couple system except adding batteries for energy storage.

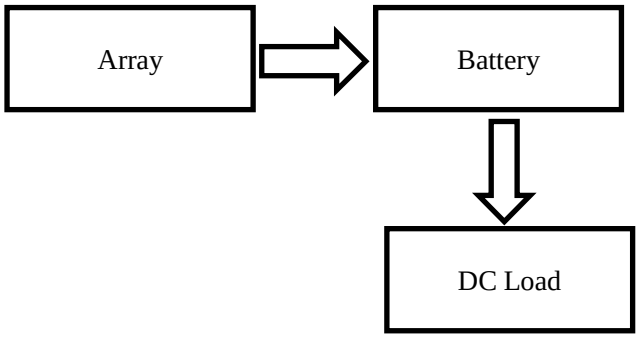

Figure 5-2 Schematic of Self- Regulated Systems

c) Charge-Controlled Systems

We know that the battery could be overcharged if there is no charge controller between power and battery. Therefore, most stand-alone systems have a charge controller device to make sure the system work safely.

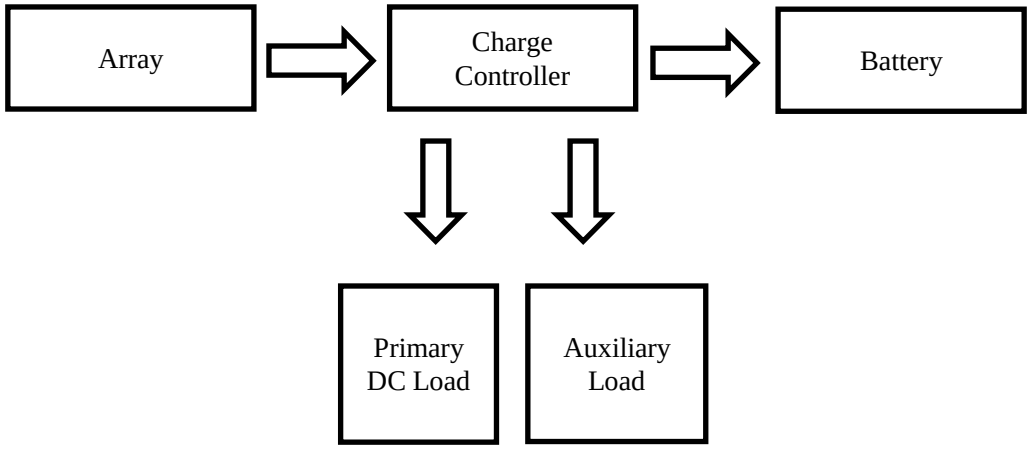

Figure 5-3 Schematic of Charge- Controlled Systems

d) Stand-Alone Systems for AC loads

When the loads are working in direct current circuit, we can choose any of the types of systems as indicated above. However, if there is an AC load, an inverter is a necessary part for stand-alone systems as indicated in Figure 5-4.

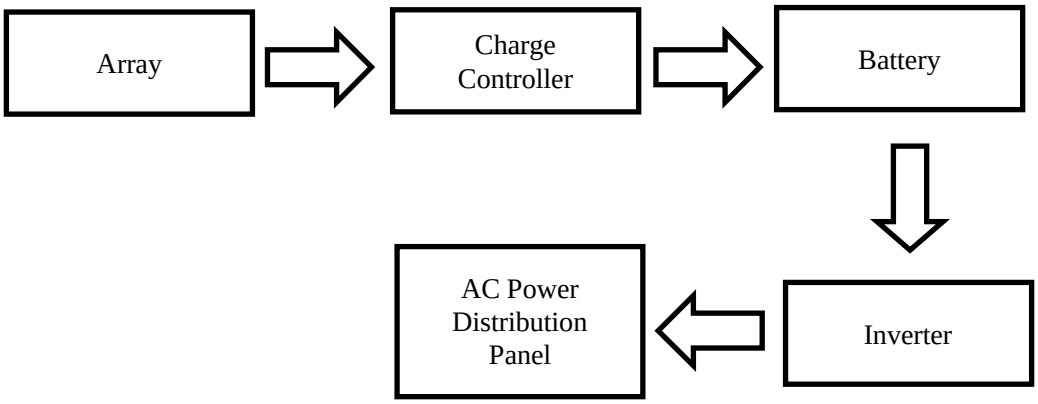

Figure 5-4 Schematic of Stand- Alone Systems for AC loads

For Utility-Interactive Systems:

Utility-Interactive system is also called grid-connected system and is a PV system that operates in parallel with and is connected to the electric utility grid.

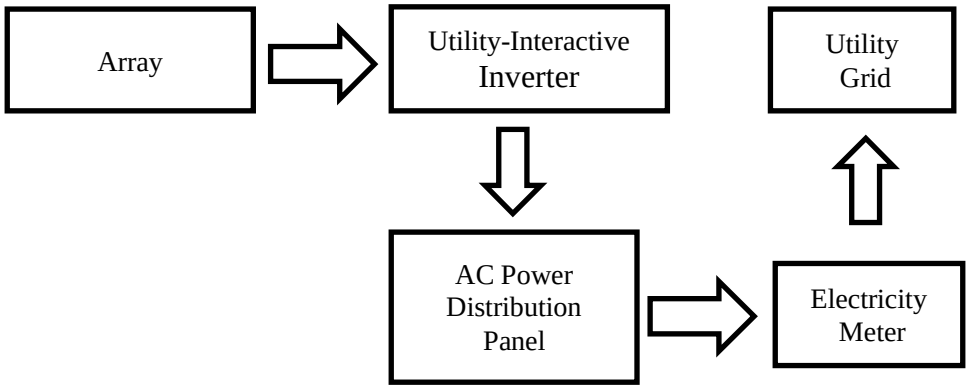

Figure 5-5 Schematic of Utility- Interactive Systems

For Hybrid Systems:

A hybrid system is a system that includes an energy source other than an array and the utility. Common energy sources used in hybrid systems include engine generators, wind turbines, or micro-hydroelectric turbines.

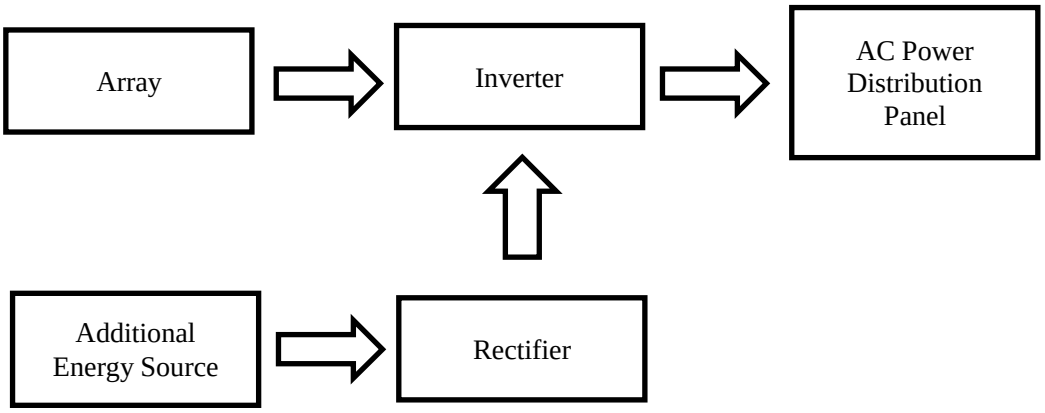

Figure 5-6 Schematic of Hybrid Systems

5.2 Solar Energy System Simulation for Household

The EIA Annual Energy Review indicates that there are 4.95 quadrillion Btu electricity consumption in the residential sector in the United States in 2010. For the commercial sector the consumption is about 4.54 quadrillion Btu and about 3.28 quadrillion Btu for the industrial sector. For transportation, the consumption is 0.02 quadrillion Btu. Note conversion factors:

$$1\text{kWh} = 3412.14\text{Btu}$$

$$1\ \text{Quad} = \text{Quads of Btu} = 10^{15}\text{Btu}$$

$$1\text{Btu} = 0.0002930711\ \text{kWh}$$

Thus, the annual electrical consumption is 12,000 kWh electricity per capita in 2010 and 33 kWh per day per capita.

Here, for a typical four-person family, the daily approximate consumptions is 46 kWh.

Definition of electrical appliances by individual appliance is shown in table 5.1.

Table 5.1 Electricity daily consumption estimation for a four people family

Number	Appliances	Power	Mean Daily Use
4	Fluorescent lamps	60watt/lamp	5h/d
1	TV/Magnetoscope/PC	80watt/app.	2h/d
1	Fridge	160watt/app.	4h/d
1	Washing machine and Washer dryer	2,200watt/app.	0.5h/d
1	Water heater	4,000watt/app.	4h/d
1	Heat pump	5,000watt/app.	10h/d

Because of the low solar radiation in NYC, we use Utility-Interactive Systems as shown in Figure 5-5 in the present photovoltaic system simulation. The only thing I need do is just to change the array as our CPV/T model. The following location is used for the current case study:

Site name: New York City, Country: USA Region: North America, Latitude: N 40.78 degrees, Longitude: W 73.97 degrees.

As mentioned in chapter 4, the area of concentrating dish considered here is 30 m^2, so the diameter is 6.18 m. The area of solar panel is 4 m^2 with radius 1.13 m.

Based on the climate data for New York Central Park (observatory), we find the daily normal beam irradiation is 3.5 kWh/ $\mathrm{day}/\mathrm{m}^2$. Therefore, if the system designed here is placed in this area, the radiation coming from concentrating dish per day would be

$$3.5\,\mathrm{kWh}/\mathrm{day}/\mathrm{m}^2 \times (30-4)\mathrm{m}^2 = 91\ \mathrm{kWh/day}$$

Taking the effect of the notch filter into account, the incident radiation on the solar PV plane is 18 kWh/day and the rest of that (73 kWh/day) is reflected to the cavity receiver for thermal energy collection.

Choice of PV array:

Potential efficiency of the commercial Si based PV panels as pertinent to a wavelength selective system has been discussed in an earlier section. For a wavelength selective PV system efficiencies close to 42% are possible. When the PV efficiency is 0.42, the input radiative power for the current system will be

$$\frac{0.42 \times 18\,\mathrm{kWh}}{24\mathrm{h}} = 315\mathrm{W}$$

Shell ST40 PV systems manufactured by Shell Solar GmbH are considered. The Shell PV panel has the following parameters shown in Table 5.2:

Table 5.2 Specifications of Shell ST40

Specifications of Shell ST40	
Rated Power (W)	40
Cell Type	CIS
Price ($)	335
Open Circuit Voltage V_{oc}(V)	23.3
Short Circuit Current I_{sc}(A)	2.68
Voltage at Maximum Power V_{mp}(V)	16.6
Current at Maximum Power I_{mp}(A)	2.41
Width (mm)	328
Height (mm)	1,293
Gross Surface Area (m^2)	0.42

Economic contribution corresponding to electricity generation:

In this part, the dollar equivalent of electricity produced by CPV/T dish on a monthly basis is calculated. First, solar radiation information need to be known. Normal Beam irradiance for New York City monthly is shown in Figure 5-7.

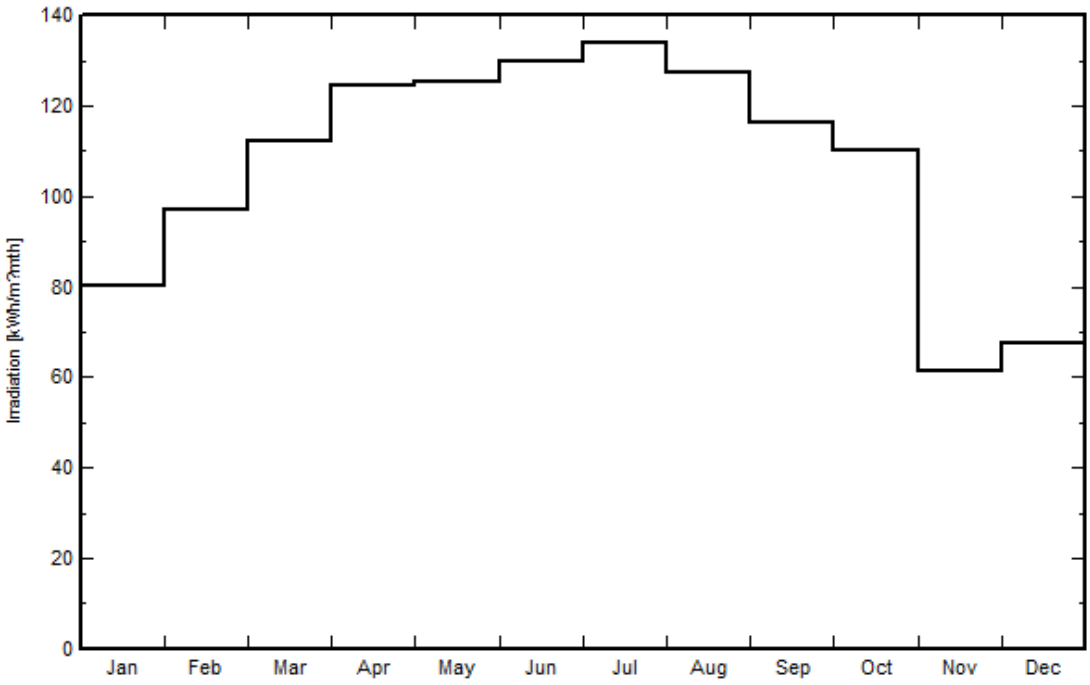

Figure 5-7 Normal beam irradiance at NYC monthly

From Table5.3, it is seen that this system can produce 2,781 kWh per year. With the cost of electrical energy (the PPL electric utilities' price) of $0.10 per kilo-watt-hour, the equivalent economic value is,.

$$2{,}781\ \text{kWh} \times \frac{\$0.10 \text{dollars}}{\text{kWh}} = \$278.10\ \text{per year}$$

Table 5.3 summarizes the amount of energy that can be captured using the wavelength selected PV system, its economic equivalence as well as the energy that is likely to be used by a typical 'family of four.'

Table 5.3 Energy produced by PV Array and consumption by a four people family monthly

Month	**Normal Beam Irradiance per day** (kWh/m^2)	**Electricity output per day** (kWh)	**Electricity consumption per day** (kWh)
1	2.58	5.58	68.3
2	3.46	7.48	68.3
3	3.62	7.83	68.3
4	4.15	8.97	29.1
5	4.04	8.74	29.1
6	4.34	9.38	29.1
7	4.33	9.36	39.1
8	4.12	8.91	39.1
9	3.88	8.39	39.1
10	3.55	7.68	29.1
11	2.04	4.41	50
12	2.18	4.71	68.3
TOTAL (per year)	1286.4	2781	16912

Economic contribution corresponding to electricity generation:

The amount of thermal energy that is collected with the current thermal receiver is first evaluated. Because of notch filter, that provides for wavelength demarked thermal energy from the solar energy that will heat the fluid can be evaluated.

The average thermal efficiency η_{th} of the hybrid PV/T systems is calculated by the relation:

$$\eta_{th} = \dot{m} c_p (T_0 - T_i)/P$$

where, P is received solar power received/incident on the dish and incident on the cavity. For the current application, the fluid mass flow

rate ($\dot{m} = \frac{dm}{dt} = (0.32 \text{ gallons per minute})$), the fluid temperature rise ($T_0 - T_i$) and the fluid specific heat C_p (4,180 $JKg^{-1}K^{-1}$ for water and 1,007 $JKg^{-1}K^{-1}$ for air)

For example, if the received solar power by the cavity receiver in January is 1812.5 W, and the thermal efficiency η_{th} is 0.9 and the inlet temperature is 25°C , thus, we can calculate the output temperature T_0:

$$T_0 = \frac{\eta_{th} G}{\dot{m} c_p} + T_i = 45\ ℃$$

which can result in heating 0.02 kg s^{-1} (approximate 0.32 GPM) water by 20°C. You could find the average output temperature monthly from Table 5.4.

Table 5.4 Received power by cavity and output temperature monthly

Month	Beam Irradiance (W/m^2)	Received power by cavity (W)	Output temperature (℃)
1	107.5	1812.5	45
2	144.2	2431.3	51
3	150.8	2542.6	52
4	173.0	2916.9	56
5	168.3	2837.7	55
6	180.8	3048.4	58
7	180.4	3041.7	58
8	171.7	2895.0	56
9	161.7	2726.4	54
10	148.0	2495.4	52
11	85.0	1433.2	40
12	90.8	1531.0	41

The area of PV array is 4 m^2 , and for the eight Shell ST40 PV panels the total cost is likely to be $2,680.

With regard to thermal energy collected and possibly used for heating water, if diesel oil is used and the price of Diesel oil is $4.30/gallon, we could evaluate how much money could be saved using this system. To be able to do that, the energy collected by the system per year is first calculated. From Table 5.2, the average normal beam solar radiation in the New York area is 1,286.4 kWh/m^2 and thus the energy captured by cavity per year can be expressed as:

$$1286.4 \times 0.86 \times 0.9 \times 0.778 \times (30 - 4) = 20,14021,689.8 \text{ kWh}$$

When diesel oil is used, it offers a net heating value of 42 MJ/kg and the density of diesel is 860 kg/m^3. Therefore, we can calculate how much energy we save from this.

$$\frac{20{,}140 \times 1000 \times 3600\text{J}}{\left(\frac{42\text{MJ}}{\text{kg}}\right) \times \left(\frac{860\text{kg}}{\text{m}^3}\right)} = 2.01\text{m}^3 = 531 \text{ gallons}$$

$$531 \text{ gallons} \times \frac{\$4.30}{\text{gallon}} = \$2{,}283$$

When electricity is used to heat water (which is a poor usage of energy!) so that we can obtain the same thermal energy, the cost savings in dollars will be:

$$20{,}140 \text{ kWh} \times \frac{0.1}{1\text{kWh}} = \$2{,}014.$$

When natural gas is to heat water, we can easily find how much does this system save in dollars as well. 1 kWh = 3,412.14Btu

$$20{,}140 \times 3412.14\text{Btu} \times \frac{\$4}{10^6\text{Btu}} = \$275.$$

The price of the dish installed is likely to be around $\$400/\text{m}^2$, the cost of solar collector will be about $12,000. .

Therefore, the total cost of the CPV/T system is $14,680. The economic equivalence of the electrical and thermal energy garnered from this CPV/T dish is in the range of ($278 + 275) = $553 or to ($278 + $2,283) =$2,561. The linear payback period for this is likely to be in the range of 5.7 to 26.5 year depending on the type of fossil fuel it is compared and the effective rate use for the electricity. If the user is ‘all-electric’ and the rates are $0.32/kWh as in Hawaii or the PPA rates used for calculations in Germany, the payback period will be significantly shorter.

CHAPTER 6. CONCLUSIONS

Although an extensive amount of research on PV/T has been carried out over the last 25 years, little is reported in the literature about the use of spectrally selective use of solar energy to develop PV/T systems. This work is an attempt to fill the void in that field with the use of spectrally differentiated energy that is used for electrical energy generation with the rest of the energy collected as thermal energy. A CPV/T system with a solar collector area of 6.2 m diameter, 30 m^2 area along with 2.3 m diameter, 4 m^2 Si solar PV panel with spectral selection of radiation for the two devices.

The theoretical efficiency of a solar cell is difficult to calculate from first principles. It depends on so many factors that affect the performance of the cells such as irradiance, and temperature and cost. A detailed calculation for electrical efficiency based on the spectrally selected solar energy has been developed and presented in an earlier section of this work. Calculations using Mathematica software indicates that electrical efficiency of non-concentrating PV system is about 55 percent using the Shockley-Queisser approach and 39 percent using a device-based method.

Four important parameters have been identified as important since they will influence the PV cell efficiency. The first one is the open-circuit voltage, which is determined by the properties of the semiconductor. The second one is short-circuit current density, which is greatly affected by the solar irradiance as well as the charge dissipation near the (p-n) junctions. Along with cost the last important parameter is the fill factor, which is reduced by the recombination in the depletion region. Based on NREL's data for solar radiative spectrum (AM 1.5G) and intensity (~1,000 W/m^2), and the efficiency evaluated here of CPV cells is about 42 percent using device-based approach.

For Si based PV cells, the band gap is about 1.11 eV. This corresponds to photon wavelengths from 800 nm to 1120 nm that can be used for PV use. Photons with longer wavelengths are not energetic enough to displace electrons and useless for Si PV applications while photons below 800 nm wavelength have energies much larger than (>1.11 eV) needed with the excess energy showing up as heat. Thus solar radiation below 800 nm as well as beyond 1,100 nm, photons are reflected into a cavity receiver for thermal collection.

As we split the solar spectrum into two parts, about 78 percent of the energy is collected solar thermal energy will be reflected and captured in a cavity receiver in which energy could be used to heat water. Calculations are done for New York City where the average normal beam insolation is 1,286 kWh/m^2 per year. Using the 42 percent CPV electrical efficiency and for the area of solar cells of 4 m^2, about 2,781 kWh electricity per year is possible. This is approximately 22 percent of the 13,793 kWh electrical energy used by the application from the grid. The thermal energy collected is part of the 78 percent (850 nm< and >1,100 nm) of the solar energy. The cavity receiver collects about 69 MMBtu or 20,140 kWh equivalent of solar thermal energy per year from the 30 m^2 dish.

Simulations of a CPV/T 30 m^2 dish with a 4 m^2 of PV area for a CPV/T system in the context of energy consumption by a four people family in New York City shows that the dish can in a year produce 2,781 kWh of electricity and thermal energy 69 MMBtu (or 20,140 kWh equivalent) while the average electricity consumption is 16,912 kWh per year. The approximate total cost of this CPV/T system is likely to be $14,680 and the linear payback period for the dish could be anywhere between 5.7 and 26.5 years depending on the cost of the energy and the types of energy used.

REFERENCE

1. Philips and Kenneth, J. H., 1995, *Guide to the Sun*, Cambridge University Press, pp. 47-53.

2. Luque, A., and Hegedus, S., 2011, *Handbook of Photovoltaic Science and Engineering*, John Wiley & Sons, Hoboken, NJ.

3. Beckman, W. A., and Duffie, J. A., 2006, *Solar Engineering of Thermal Processes*, John Wiley & Sons, Hoboken, NJ.

4. Dunlop, J. P., 2009, *Photovoltaic Systems*, American Technical Publishers, Orland Park, IL.

5. Incropera, F. P. and DeWitt, D. P., 1990, *Introduction of Heat Transfer*, 3rd ed, John Wiley & Sons, New York.

6. Hodge, B. K., 2010, *Alternative Energy Systems and Applications*, John Wiley & Sons, Hoboken, NJ.

7. Sze, S. M., 1981, *Physics of Semiconductor Devices*, John Wiley & Sons, Hoboken, NJ.

8. Charalambous, P. G., Maidment, G. G., Kalogirou, S. A., and Yiakoumetti, K., 2007, "Photovoltaic Thermal (PV/T) Collectors: A Review," Appl. Thermal Engineering, **27**(2-3), pp. 275-286.

9. Hottel, H. C., and Woertz, B., 1942, "Performance of Flat-Plate Solar Heat Collectors," Trans. ASME, **64**, 91.

10. Nelson, J., 2003, *the Physics of Solar Cells*, Imperial College Press, London, UK, Chap. 2.

11. Shockley, W., and Queisser, H. J., 1961, "Detailed Balance Limit of Efficiency of p-n Junction Solar Cells," J. Appl. Phys., **32**(3), pp. 510-519.

12. Campbell, P., and Green, M. A., 1986, "The Limiting Efficiency of Silicon Solar Cells under Concentrated Sunlight," IEEE Trans. Electron Devices, **33**(2), pp. 234-239.

13. Sinton, R. A., Kwark, Y., Gan, J. Y., and Swanson, R. M., 1986, "27.5-Percent Silicon Concentrator Solar Cells," IEEE Electron Device Letters, **7**(10), pp. 567-569.

14. Tripanagnostopoulos, Y., Nousia, T., Souliotis, M., and Yianoulis, P., 2002, "Hybrid Photovoltaic/Thermal Solar Systems," Solar Energy, **72**(3), pp. 217-234.

15. Green, M. A., 2003, *Third Generation Photovoltaics*, Springer, New York, Chap. 4.

16. Zhang, Y., Ding, D., Johnson, S. R., and Lim, S. H., 2010, “A Semi-Analytical Model and Characterization Techniques for Concentrated Photovoltaic Multijunction Solar Cells,” *Optics for Solar Energy*

17. Wolf, M., 1980, “Updating the Limit Efficiency of Silicon Solar Cells,” IEEE Trans. Electron Devices, **27**(4), pp. 751-760.

18. Tiedje, T., Yablonovitch, E., Cody, G. D., Brooks, B. G., 1984, “Limiting Efficiency of Silicon Solar Cells,” IEEE Trans. Electron Devices, **31**(5), pp. 711-716.

19. Bergene, T., 1995, “Model Calculations on A Flat-Plate Solar Heat Collector with Integrated Solar cells,” Solar Energy, **55**(6), pp. 453-462

Vita

Suming Guo was born on September 3, 1985, in Jiangxi Province, China. He lived in Beijing and graduated from Renbishi High School in 2005. Later, he took National Entrance Examination for Colleges and enrolled in Beijing Institute of Technology. He completed his Bachelor of Science in Automobile Engineering in July 2009. He came to United States in July 2010 and joined Lehigh University to pursue graduate study in the field of Mechanical Engineering. He expects to earn his Master of Science degree in September 2012.